Supplementary Information

Lead-free double perovskite $Cs_2AgBiBr_6$/BiOBr S-scheme heterojunction with enhanced Bi-Br-Bi coordination for photocatalytic CO_2 reduction

Jianwen Zhang [a, #], Chunling Hu [b, #], Hailong Li [a, *], Qi Zhang [a], Kangning Xue [a, b], Ji Zhou [a], Long Wang [a, b], Junfeng Gao [a, c *], Juan Hou [a *]

a. State Key Laboratory of Advanced Energy Storage Materials and Technology, College of Sciences, Shihezi University, Shihezi 832003 China

b. State Key Laboratory Incubation Base for Green Processing of Chemical Engineering, School of Chemistry and Chemical Engineering, Shihezi University, Shihezi 832003 China

c. State Key Laboratory of Structural Analysis for Industrial Equipment & School of Physics, Dalian University of Technology, Dalian, 116024 China

Co-first authors of the article

*Corresponding authors.

E-mail: well09131015@shzu.edu.cn (H. Li); gaojf@dlut.edu.cn (J. Gao); hjuan05@sina.com (J. Hou).

1. Chemicals and materials

The detailed nomenclature, specifications, and manufacturers of the chemicals and materials are listed in Table S1. All drugs were procured and utilised in their original state, without undergoing any form of purification.

2. Preparation of BiOBr nanoflowers (BOB NF)

$Bi(NO_3)_3 \cdot 5H_2O$ (970 mg) and CTAB (350 mg) are to be dissolved in 12 mL of ethylene glycol and 48 mL of tert-butanol. Subsequently, the mixture should be subjected to vigorous stirring for a period of three hours and ultrasonic treatment for a period of 30 minutes. The solution should then be transferred into an 80 mL Teflon-lined stainless steel autoclave. Subsequently, the mixture was subjected to high-pressure steam heating at 160°C for 8 hours, cooled to room temperature, and washed by alternating centrifugation with water and ethanol. The sample was then subjected to vacuum drying at a temperature of 60°C for a period of 24 hours.

3. Preparation of $Cs_2AgBiBr_6$ nanosheets (CABB NS)

825 mg Cs_2CO_3 and 10 mL oleic acid were placed in a 25 mL three-neck flask. The mixture was degassed under vacuum at 100°C for 30 min, then heated to 150°C for 1 h under a stream of N_2. The reaction solution was subsequently cooled to room temperature for further use. Subsequently, 45 mg $BiBr_3$, 34 mg $AgNO_3$, 100 μL HBr, 1 mL oleic acid, 1 mL oleylamine, and 4 mL 1-octadecene were added to the flask. The process of forming a homogeneous solution by heating and degassing at 120°C, followed by heating to 200°C under N_2 protection, is a critical step in the overall procedure. Subsequently, the reaction mixture was cooled to room temperature. The addition of 0.3 ml of Cs oleate precursor solution was undertaken to induce the nucleation of $Cs_2AgBiBr_6$ cluster-based nanosheets. Subsequently, the reaction mixture was reheated to 230°C for a period of 10 minutes, after which the heating jacket was detached in order to quench the reaction. The samples were then washed and subjected to centrifugation, followed by vacuum drying at 60°C for 12 hours.

4. Instrumentations:

XRD patterns were obtained using the Bruker diffractometer (Bruker D8 Advance, Germany) by Cu Kα radiation (λ = 0.15418 nm) and a scan range of 10-80 degrees. During the XRD test, the scan speed was 5° per minute. The surface potential of BOB and CABB in ethanol was measured using a Nanoparticle Size and Zeta Potential Analyzer (DLS) (Malvern Zetasizer Nano ZS90, Britain). SEM images were recorded on a Hitachi SU-8010 scanning electron microscope. TEM and HR-TEM images were obtained on a JEOL JEM-F200 (Japan). UV-vis diffuse reflectance spectra (DRS) were obtained on a Cary 5000 spectrophotometer (Agilent) using $BaSO_4$ as the reflectance standard. XPS measurements were carried out on an ESCALAB Xi+ X-ray photoelectron spectrometer (Thermo scientific), calibrated by the value of adventitious C 1s peak (284.8 eV). The corresponding XPS spectra were fitted using Avantage software. Photoluminescence (PL) spectra and Time time-resolved photoluminescence emission spectra (TRPL) were obtained on a Edinburgh FLS1000 (Britain) under 404 nm excitation. PL lifetimes were determined by assuming triple exponential decay kinetics: $A_1 \exp(-t/\tau_1)+A_2 \exp(-t/\tau_2)+A_3 \exp(-t/\tau_3)$, with $\tau_{avg} = \Sigma A_i\tau_i^2/\Sigma A_i\tau_i$, where i corresponds to the i^{th} component of a given multiexponential decay process.

5. Photoelectrochemical measurements

Photocurrent measurements were performed in a standard three electrode cell with the assembled photoelectrodes (BOB, CABB, or BOB/CABB on FTO glass (1 cm^2), as the working electrode, a platinum foil as the counter electrode, and a saturated Ag/AgCl electrode as the reference electrode. The electrolyte is a 0.1 M solution of $TBAPF_6$ in acetonitrile: ethyl acetate (1:9). The working electrode was prepared as follows: The working electrodes were prepared as follows: 10 mg of catalyst was dispersed in 1.98 mL of ethyl acetate containing 20 μL Nafion. Then 500 μL of the catalyst dispersion was dropped onto a FTO glass with an area of 2.5 cm^2 to form a uniform thin film. Excess material is scraped off, leaving 1 cm^2 of film. The photocurrents were recorded on a Zahner electrochemical workstation (Autolab, Switzerland) under irradiation from a 300 W Xe lamp (AM 1.5G, 150 mW cm^{-2}) at a potential of -0.4V. Electrochemical impedance spectroscopy (EIS) data were obtained at the open circuit potential using a

frequency ranged from 10^5 Hz to 10^{-2} Hz. The corresponding Nyquist diagrams were fitted using ZView2 software.

6. Interface Electric Field Strength Calculation

To investigate the presence of an internal electric field at the interface, we used the equation proposed by Kanata et al. [1], conducting a qualitative measurement of photocatalyst intensity based on the method described by Liu et al. [2]

$$Fs = \sqrt{\left(-\frac{2Vs\rho}{\varepsilon\varepsilon_0}\right)}$$

Where, *Fs* is the internal electric field magnitude, *Vs* is the surface voltage, ρ is the surface charge density, ε is the low-frequency dielectric constant, and ε_0 is the permittivity of free space. As ε and ε₀ are constants, it is sufficient to measure the surface voltage (V_s) and surface charge density (ρ) in order to quantitatively compare the interfacial electric field strengths of BOB, CABB, and BOB/CABB. Accordingly, the surface voltage of the sample is evaluated through the means of open-circuit potential (Fig. S7a-c). The surface current density [3]. is calculated by subtracting the integral value of the simultaneous steady-state photocurrent density from the transient photocurrent density (Fig. S7d-f). The built-in electric field strengths of CABB and BOB/CABB are quantified by defining the BOB with the minimum interfacial electric field strength as the unit.

7. Average rate of CO_2 reduction products and CO electron selectivity

The yield rate of product: $R_{product} = \sum_{i=1}^{t} (R_i/i)/t$

The electron selectivity of CO: $CO\ (\%) = R_{CO}/(R_{CH4} + R_{CO} + R_{H2}) \times 100\%$

Where R_i is the amount produced per hour by 1 g of catalyst, and t is the total reaction time.

8. Calculation of band edge positions and redox potentials

The work function as an important method for determining the thermo-dynamic ability to generate the CO_2/CO radicals, and is used to determine the edge position of the valence band maximum (VBM) and conduction band minimum (CBM), which was

evaluate band edge position of generation of CO. It is well known that a catalyst can reduce CO_2 to CO only when the CBM position is below the CO_2/CO reduction potential of -0.10 V vs. NHE. Therefore, the band edge positions of the CBM and VBM in the BOB/CABB system can be determined using the following equation [4].

E_{VBM} (eV) = - Φ + 0.5 Eg

E_{CBM} (eV) = - Φ - 0.5 Eg

$E_{CBM/VBM}$ (V) = - $E_{VBM/CBM}$ (pH = 7) - 4.5

Where Φ is the work function, Eg is the band gap, and $E_{CBM/VBM}$ is potential versus NHE (pH=7.0, 0 V vs. NHE ~ -4.5 eV).

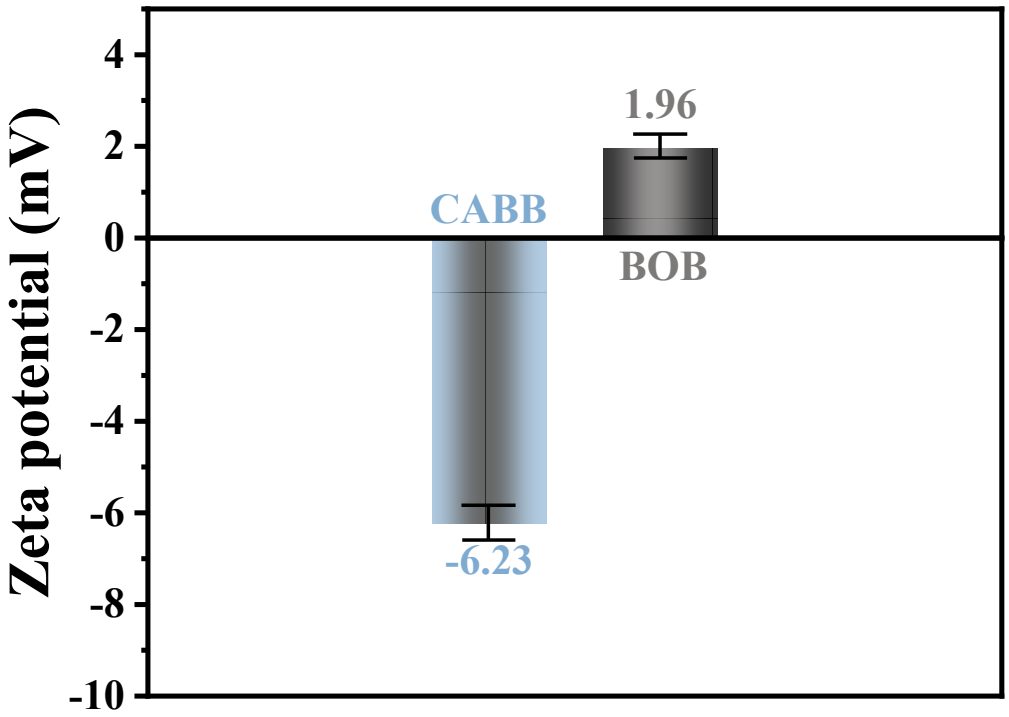

Fig. S1. Zeta potential of CABB and BOB.

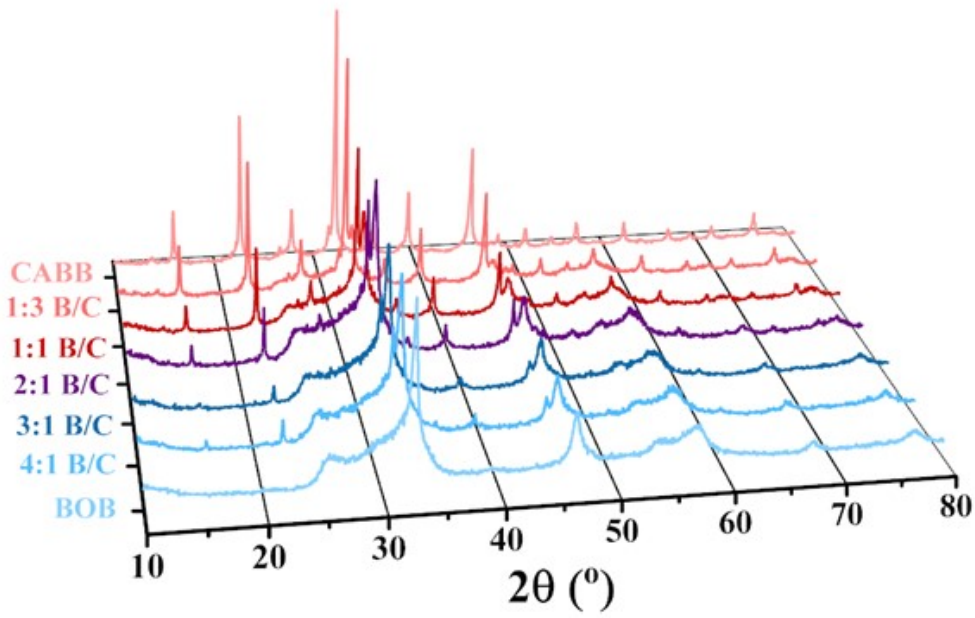

Fig. S2. XRD of BOB/CABB at Different Blending Ratios

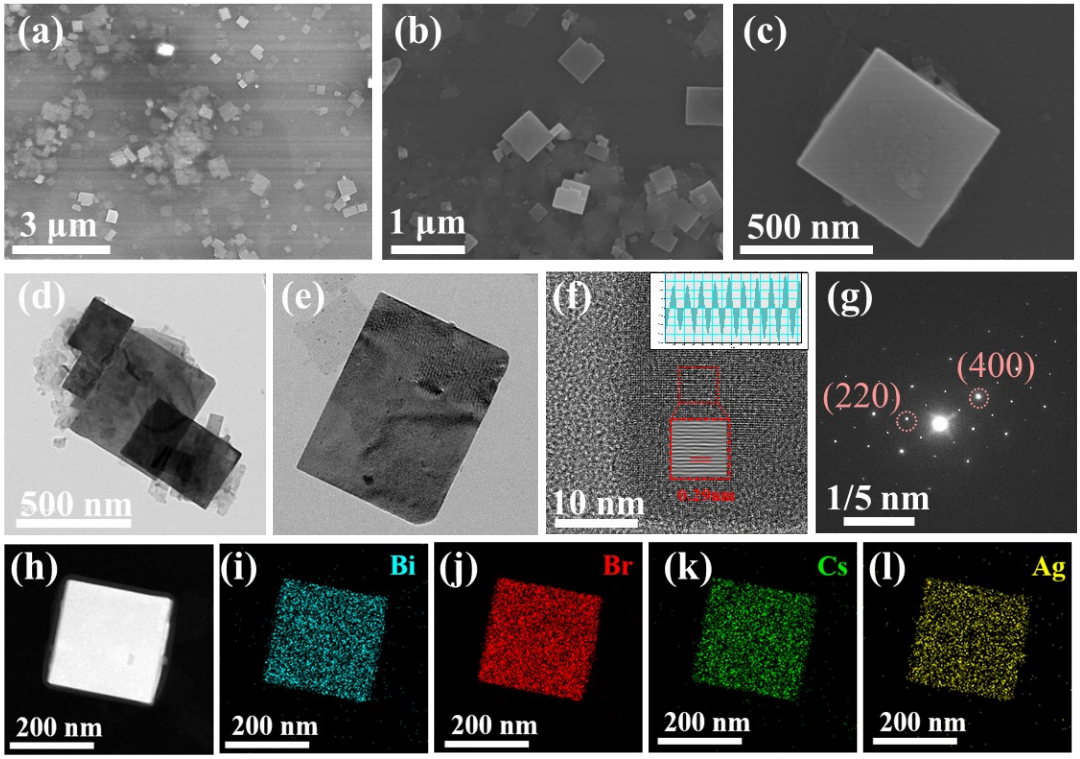

Fig. S3. CABB (a–c) SEM images, (d, e) TEM images, (f) HRTEM image, (g) Lattice diffraction pattern, and (h–l) TEM mapping.

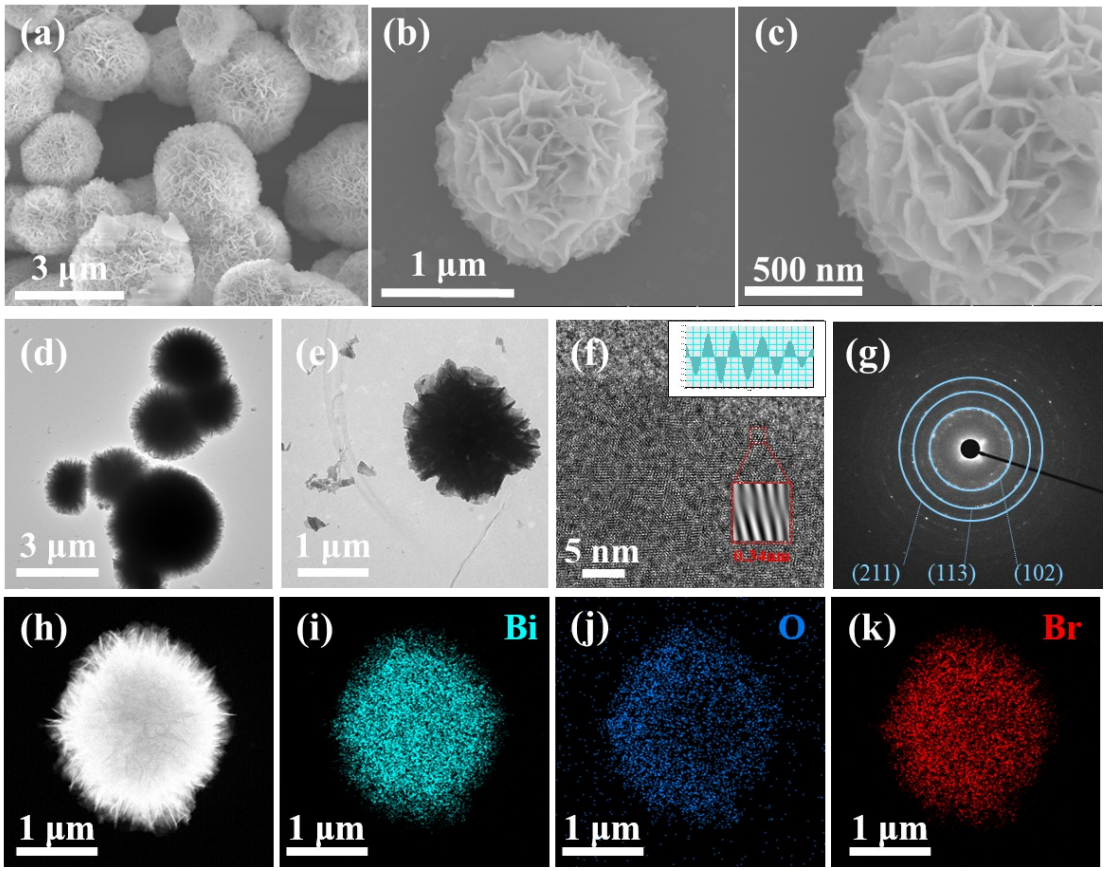

Fig. S4. BOB (a–c) SEM images, (d, e) TEM images, (f) HRTEM image, (g) Lattice diffraction pattern, and (h–k) TEM mapping.

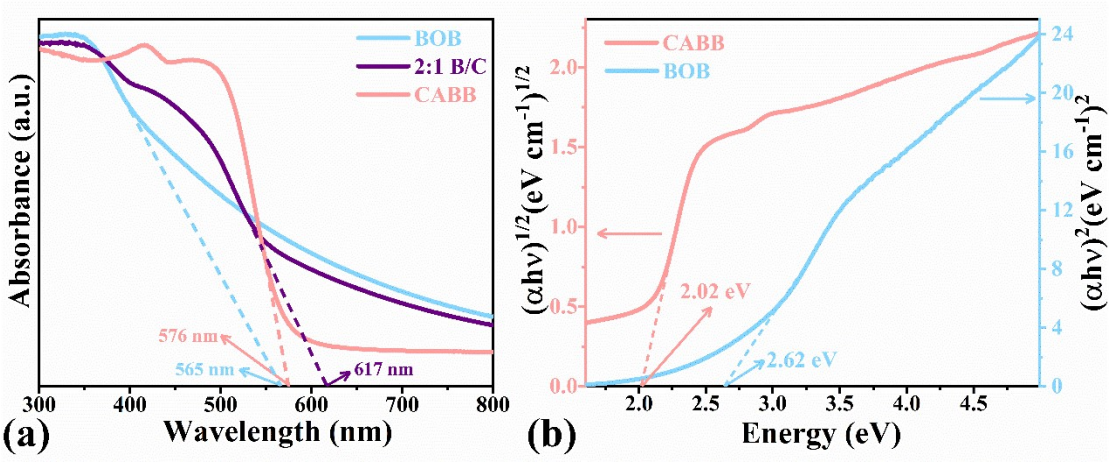

Fig. S5. (a) UV-vis DRS spectra and (b) tauc plot of BOB, CABB, and BOB/CABB

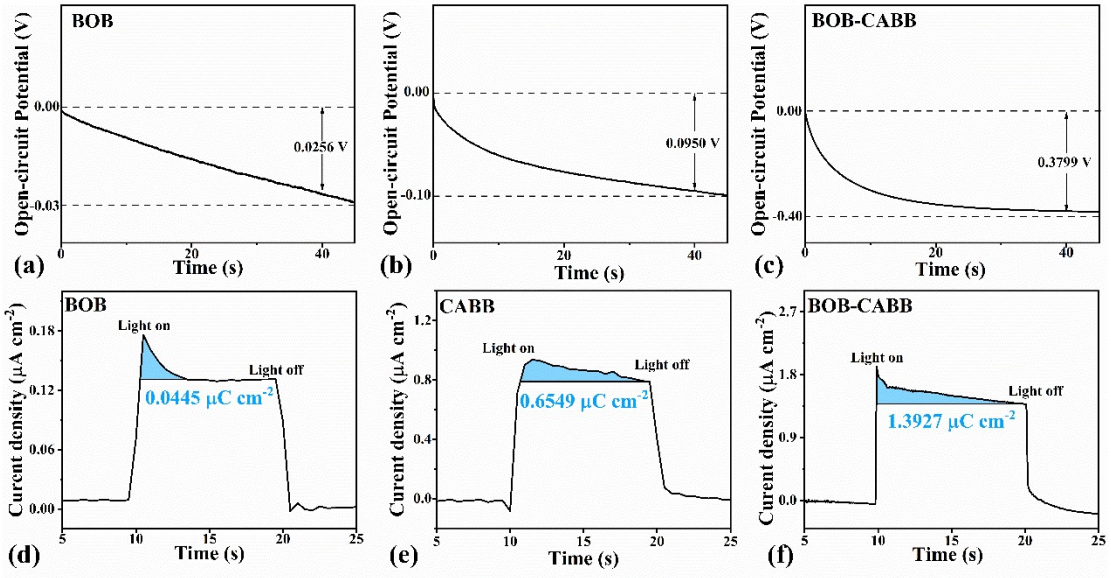

Fig. S6. (a-c) The open-circuit potential and (d-f) the transient photocurrent density of BOB, CABB, BOB/CABB.

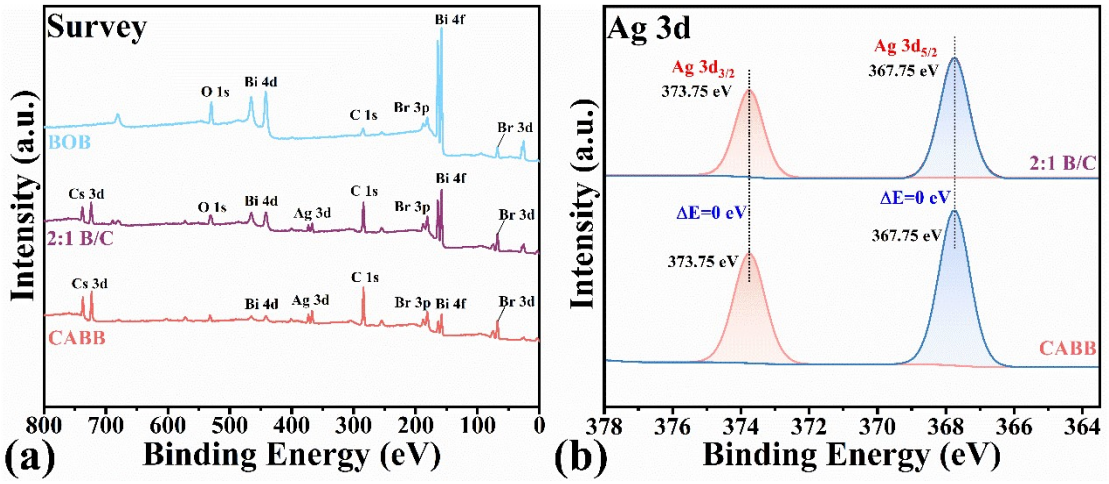

Fig. S7. XPS spectra of (a) Survey and (b) Ag 3d in BOB, CABB and BOB/CABB

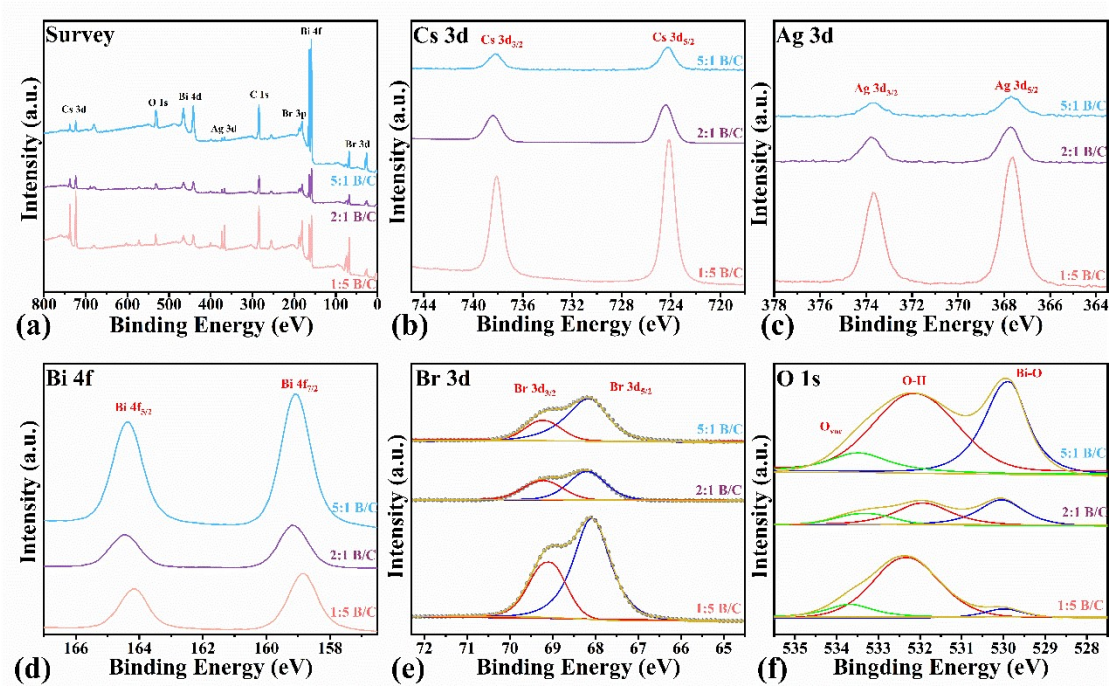

Fig. S8. XPS spectra of 1:5, 2:1, 5:1BOB/CABB

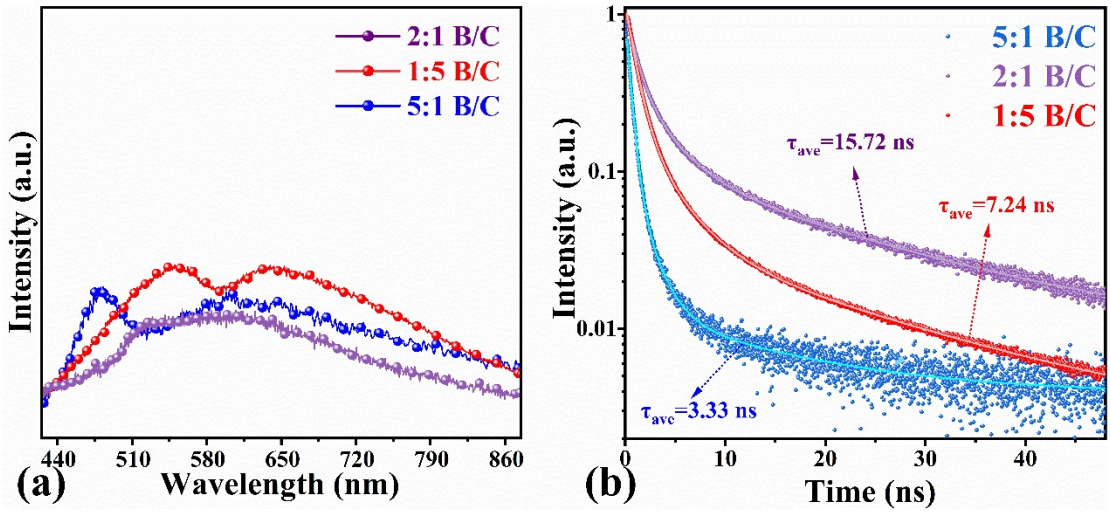

Fig.S9. PL (a) and TRPL (b) of 1:5, 2:1, 5:1BOB/CABB

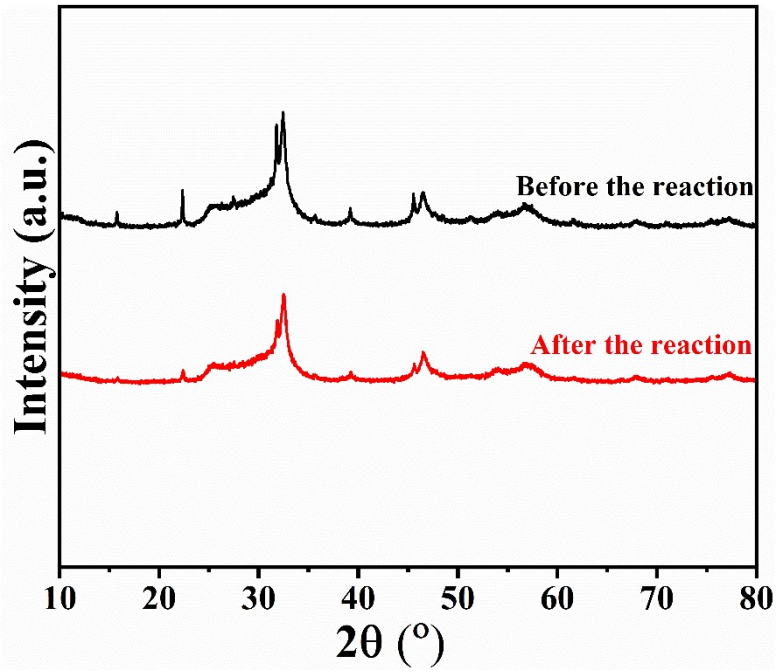

Fig.S10. XRD before and after reaction

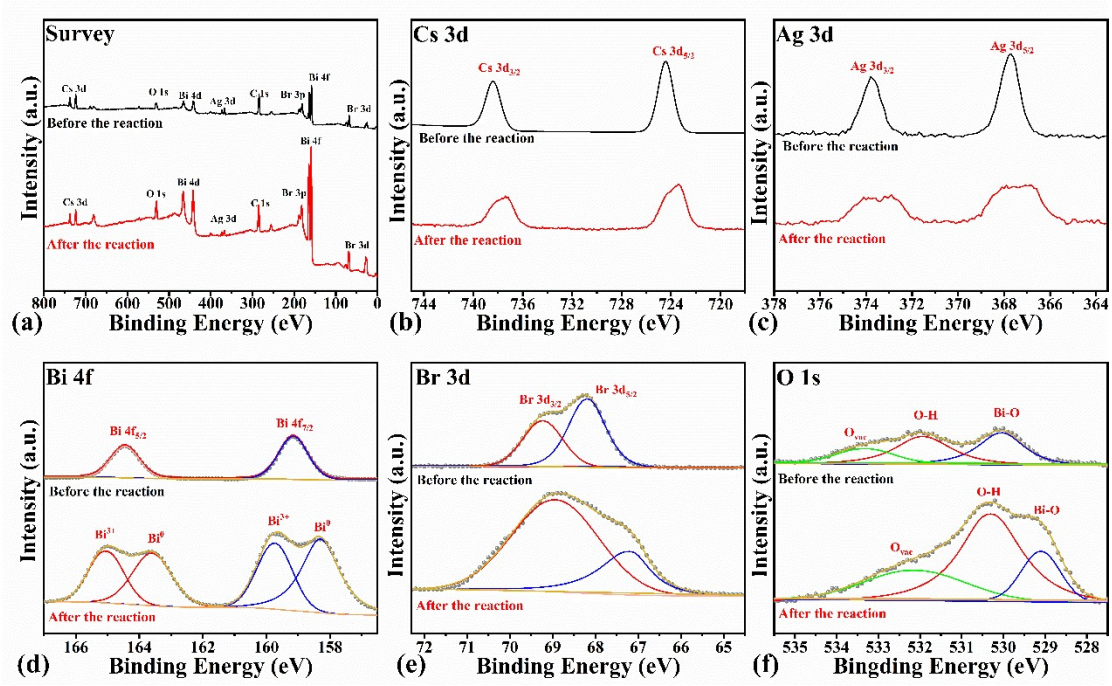

Figure S11. High-resolution XPS spectra of fresh and used 2:1 BOB/CABB heterojunction after four photocatalytic cycles.

Table S1. Chemicals and material details

Chemical	Molecular formula	Specifications	Manufacturer
Bismuth tribromide	$BiBr_3$	99.99% metal basis	Shanghai Aladdin Biochemical Technology Co., Ltd.
Silver nitrate	$AgNO_3$	AR	Shanghai Aladdin Biochemical Technology Co., Ltd.
Cesium carbonate	Cs_2CO_3	99.9% metals basis	Shanghai Aladdin Biochemical Technology Co., Ltd.
1-Octadecene	$C_{18}H_{36}$	＞90%	Shanghai Macklin Biochemical Co.,Ltd.
Hydrobromic acid	HBr	ACS, 48%	Shanghai Aladdin Biochemical Technology Co., Ltd.
Oleic acid	$C_{18}H_{34}O_2$	85%	Shanghai Aladdin Biochemical Technology Co., Ltd.
Oleylamine	$C_{18}H_{37}N$	Technical grade, 70%	Shanghai Aladdin Biochemical Technology Co., Ltd.
Toluene	C_7H_8	≥99.5%	Chengdu Kelon Chemicals Co. , Ltd.
Bismuth nitrate pentahydrate	$Bi(NO_3)_3 \cdot 5H_2O$	AR	Shanghai Macklin Biochemical Co.,Ltd.
Hexadecyl trimethyl ammonium Bromide (CTAB)	$C_{19}H_{42}BrN$	99%	Shanghai Aladdin Biochemical Technology Co., Ltd.
Ethylene glycol	$C_2H_6O_2$	≥98%	Shanghai Aladdin Biochemical Technology Co., Ltd.
Tert-Butanol	$C_4H_{10}O$	AR	Shanghai Aladdin Biochemical Technology Co., Ltd.
Ethanol absolute	C_2H_6O	AR	Tianjin Fuyu Chemical Co. , Ltd.
Ethyl acetate	$C_4H_8O_2$	AR	Shanghai Aladdin Biochemical Technology Co., Ltd.
Acetonitrile	CH_3CN	AR	Shanghai Aladdin Biochemical Technology Co., Ltd.
Nafion	$C_9HF_{17}O_5S$	AR	Sigma-Aldrich(Shanghai)Trading Co.,Ltd

Photocatalysts	**Light soure**	**Reaction system**	**Products of CO rate (μmol g^{-1} h^{-1})**	CO electron selectivity (%)
$Cs_2AgBiBr_6$/NiFe-LDH [5]	45 mW 405 nm laser diode	Ethyl acetate	37.65	53.90
$Cs_2AgBiBr_6$/Bi_2WO_6 [6]	300W Xe lamp λ>420nm, 150 mW/cm^2	Acetonitrile/water	48.5	62.74
UiO-66-NH_2/$Cs_2AgBiBr_6$ [7]	300W Xe lamp AM 1.5G, 100 mW/cm^2	Gas (CO_2+H_2O)	17.24	82.31
$Cs_2AgBiBr_6$/$Ti_3C_2T_x$ [8]	300W Xe lamp λ>400nm, 150 mW/cm^2	Gas (CO_2+H_2O)	11.1	43.63
Rb-$Cs_2AgBiBr_6$ [9]	300W Xe lamp λ>420nm, 150 mW/cm^2	Gas (CO_2+H_2O)	12.7	52.26
g-C_3N_4@$Cs_2AgBiBr_6$ [10]	300W Xe lamp λ>420nm, 80 mW/cm^2	Ethyl acetate/water	35.52	69.43
$Cs_2AgBiBr_6$@C_3N_4 [11]	300W Xe lamp AM 1.5G 150 mW/cm^2	Wthyl acetate/methanol	1.76	64.71
$Cs_2AgBiBr_6$/Bi_2WO_6 [12]	300W Xe lamp AM 1.5G 100 mW/cm^2	Ethyl acetate/propan-2-ol	42.19	96.26
$Cs_2AgBiBr_6$@MCM-48 [13]	300W Xe lamp λ>420nm, 100 mW/cm^2	Ethyl acetate	31	63.08
$Cs_2AgBiBr_6$/Sr_2FeNbO_6 [14]	300W Xe lamp λ>420nm, 100 mW/cm^2	Gas-solid	50.00	82.48
Cu-$Cs_2AgBiBr_6$ [15]	300W Xe lamp λ>420nm, 100 mW/cm^2	Gas (CO_2+H_2O)	23.73	95.19
BiOBr/$Cs_2AgBiBr_6$ [This work]	300W Xe lamp AM 1.5G, 150 mW/cm^2	Gas (CO_2+H_2O)	**61.10**	**98.17**

1. T. Kanata, M. Matsunaga, H. Takakura, Y. Hamakawa and T. Nishino, *Journal of Applied Physics*, 1990, **68**, 5309–5313.
2. Z.-L. Liu, Y.-F. Mu, X.-R. Li, Y.-X. Feng, M. Zhang and T.-B. Lu, *Applied Catalysis B: Environment and Energy*, 2025, **366**, 125012.
3. F. Le Formal, K. Sivula and M. Grätzel, *The Journal of Physical Chemistry C*, 2012, **116**, 26707–26720.
4. B. Jing, Z. Ao, W. Zhao, Y. Xu, Z. Chen and T. An, *Journal of Materials Chemistry A*, 2020, **8**, 20363–20372.
5. X. Fu, Q. Chen, Y. Zhang, F. Yu, J. Pan and X. Yang, *Chemical Engineering Journal*, 2025, **524**, 169021.
6. H. Wang, X. Wang, P. Hu, T. Liu, B. Weng, K.-h. Ye, Y. Luo and H. Ji, *Applied Catalysis B: Environment and Energy*, 2024, **351**, 123956.
7. N. Li, Y.-L. Ma, H.-J. Zhang, D.-Y. Zhou, B.-L. Yao, J.-F. Wu, X.-P. Zhai, B. Ma, M.-J. Xiao, Q. Wang and H.-L. Zhang, *Materials Today Chemistry*, 2024, **41**, 102306.
8. Z. Zhang, B. Wang, H.-B. Zhao, J.-F. Liao, Z.-C. Zhou, T. Liu, B. He, Q. Wei, S. Chen, H.-Y. Chen, D.-B. Kuang, Y. Li and G. Xing, *Applied Catalysis B: Environmental*, 2022, **312**, 121358.
9. Z. Chen, X. Jiang, H. Xu, J. Wang, M. Zhang, D. Pan, G. Jiang, M. Z. Shahid and Z. Li, *Small*, 2024, **20**, 2401202.
10. W. Xiong, Y. Dong and A. Pan, *Nanoscale*, 2023, **15**, 15619–15625.
11. Y. Wang, H. Huang, Z. Zhang, C. Wang, Y. Yang, Q. Li and D. Xu, *Applied Catalysis B: Environmental*, 2021, **282**, 119570.
12. L. Wu, S. Zheng, H. Lin, S. Zhou, A. Mahmoud Idris, J. Wang, S. Li and Z. Li, *Journal of Colloid and Interface Science*, 2023, **629**, 233–242.
13. Z. Zhang, D. Li, Z. Dong, Y. Jiang, X. Li, Y. Chu and J. Xu, *Solar RRL*, 2023, **7**, 2300038.
14. A. Mahmoud Idris, S. Zheng, L. Wu, S. Zhou, H. Lin, Z. Chen, L. Xu, J. Wang and Z. Li, *Chemical Engineering Journal*, 2022, **446**, 137197.
15. C. Wang, W. Shen, Z. Xie, Y. Wang, Y. Ding, N. Han, M. K. H. Leung, B. Liu, Z. Zhu and Y. H. Ng, *Advanced Functional Materials*, 2025, **35**, 2503074.